AIMS Mathematics, 10(6): 13130–13150.
DOI: 10.3934/math.2025589
Received: 02 March 2025
Revised: 13 May 2025
Accepted: 23 May 2025
Published: 06 June 2025

https://www.aimspress.com/journal/Math

Research article

Mathematical analysis of tri-trophic food webs with carrying capacity and Holling-type predation using fractal-fractional Caputo derivatives

Amjad E. Hamza[1], Arshad Ali[2], Khaled Aldwoah[3,*], Hicham Saber[1], Ria Egami[4], Amel Touati[5] and Amal F. Alharbi[6]

[1] Department of Mathematics, College of Science, University of Hail, Hail 55473, Saudi Arabia
[2] Department of Mathematics, University of Malakand, Lower Dir, Chakdara 18000, Khyber Pakhtunkhwa, Pakistan
[3] Department of Mathematics, Faculty of Science, Islamic University of Madinah, Madinah 42351, Saudi Arabia
[4] Department of Mathematics, College of Science and Humanity, Prince Sattam bin Abdulaziz University, Sulail, Al-Kharj 11942, Saudi Arabia
[5] Mathematics Department, College of Science, Northern Border University, Arar 91431, Saudi Arabia
[6] Department of Mathematics, Faculty of Science, King Abdulaziz University, Jeddah 21589, Saudi Arabia

* **Correspondence:** Email: aldwoah@iu.edu.sa.

Abstract: This research investigated a tri-trophic food chain model, incorporating carrying capacity and Holling-type predation, formulated using the fractal-fractional Caputo derivative. The four equilibrium states—trivial, prey-only, prey-predator, and coexistence—presented and their stability was discussed. Existence and uniqueness of solutions were established using Schaefer's and Banach's fixed point theorems. Also, stability requirements in the sense of Hyers-Ulam (H-U) were investigated. Numerical simulations were performed using the extended numerical method of Adams-Bashforth-Moulton (ABM), and comparative results were graphically presented to demonstrate the impact of varying fractal-fractional orders. A sensitivity analysis revealed how perturbations in individual parameters influence the model's outcome. The model accounts for memory and hereditary effects in ecological interactions. The proposed method enhances accuracy, stability, and convergence for long-time simulations compared to classical models.

Keywords: tri-trophic food chain models; carrying capacity; Holling type predation; equilibrium points, existence and stability analysis; numerical analysis
Mathematics Subject Classification: 26A33, 34A08, 34A12

1. Introduction

The majority of prey-predator models focus on interactions between one or two species. For example, Hsu [1], Hsu and his co-researchers [2], and Saunders and his co-researchers [3] have developed several competition models involving two species and a resource within a chemostat. Yorke et al. presented a network-based model [4]. Food webs were regarded as energy filters by Hubbell [5] and May [6]. General discussions on the ecological behavior of food webs were provided by Conrad [7], Gallopin [8], Kerner [9], and Rosenzweig [10]. De Angelis [11] examined the connection between food webs and stability. Recently, [12] examined a diffusive predator-prey model incorporating non-local competition and a Beddington-DeAngelis-type functional response. Similarly, Zhu et al. [13] examined a diffusive predator-prey model incorporating non-local competition and the fear effect.

On other hand the dynamics of a tri-trophic food web model can be significantly more complex, as demonstrated by mathematical developments [14, 15]. Analyzing how three species are connected to form a food chain is a common approach to mathematically and biologically understanding population dynamics. Tri-trophic food chains, comprising prey, intermediate predator, and top predator species, represent a foundational structure in ecological modeling. These systems are instrumental in analyzing energy transfer, species interactions, and population regulation mechanisms. In conventional food chains, the middle predator feeds on the basal prey, while the apex predator feeds on the middle predator. Mathematical models that simulate interactions between three species have attracted considerable attention. Rescigno and his co-author [16] examined the most general Kolmogorov-type model and provided some geometrical interpretations of equilibrium as well as possible outcomes. The food-chain model studied by Hausrath [17] is a perturbed Lotka-Volterra model, but in this case, the middle level is not the only trophic level capable of reaching the highest level. He proved that the model admits a perturbed equilibrium that is asymptotically stable. In [18], using fractional-order derivatives, Seralan et al. investigated the dynamics of a three-species food chain model with a vigilance effect. In [19], Pal et al. studied a three-species food chain model involving a generalist predator with a fear effect.

In population biology, the maximum population size or density that an environment can support is referred to as the carrying capacity. The fundamental idea is that population growth follows a logistic pattern, meaning that as the population approaches its carrying capacity, the growth rate slows down. Carrying capacity is widely applied in various fields of mathematical biology, including conservation biology, ecological modeling, epidemiology, and population dynamics. A significant body of literature examines the carrying capacity of a species [20–23].

In [24], the authors investigated the following ordinary-order mathematical tri-trophic food web model with carrying capacity:

$$\begin{cases} u' = u\left[\xi_1\left(1 - \dfrac{u}{K}\right) - \xi_{12}v\right], \\ v' = v\left(\xi_2 + \xi_{21}u - \xi_{23}w\right), \\ w' = w(-\xi_3 + \xi_{32}v), \\ u(0) = g_1, v(0) = g_2, w(0) = g_3. \end{cases} \tag{1.1}$$

Model (1.1) has been modified by involving Holling-type predation of the first predator on the prey as

presented by [24]:

$$\begin{cases} u' = u\left[\xi\left(1-\dfrac{u}{K}\right)-\dfrac{\varsigma v}{1+au}\right], \\ v' = v\left(-\theta+\dfrac{b\varsigma u}{1+au}-\varepsilon w\right), \\ w' = w(-\kappa+c\varepsilon v), \\ u(0)=g_1, v(0)=g_2, w(0)=g_3. \end{cases} \tag{1.2}$$

The Holling-type predation refers to a type of predator-prey interaction modeled by the Canadian biologist C.S. Holling. It plays a crucial role in understanding predator-prey interactions and dynamics, the impact of predators on prey populations, and ecosystem stability and resilience.

Classical mathematical models typically assume logistic growth for the prey population and incorporate functional responses such as Holling type-II or type-III to account for predation saturation. Several studies (see, for instance, [18, 19, 24, 25]) have rigorously investigated the stability properties, bifurcation scenarios, and chaotic dynamics of such systems under various ecological conditions. However, the majority of the aforementioned models are based on integer-order differential equations, which inherently neglect memory and hereditary characteristics often observed in biological processes. This limitation reduces their capacity to accurately model long-term ecological behavior. Although fractional-order models based on Caputo or Riemann-Liouville derivatives have been explored to some extent, very few investigations have addressed the joint role of memory and fractal geometry in ecological contexts. To overcome this shortcoming, the present study introduces memory effects by employing a fractal-fractional differential operator, thereby enhancing the realism and descriptive power of tri-trophic models. We reformulate the food-chain model (1.2) and investigate its existence and stability in the sense of the fractal-fractional Caputo (FF-Caputo) derivative, as given by

$$\begin{cases} {}^{FFC}D^{\zeta,\Lambda}u(t) = u\left[\xi\left(1-\dfrac{u}{K}\right)-\dfrac{\varsigma v}{1+au}\right], \\ {}^{FFC}D^{\zeta,\Lambda}v(t) = v\left(-\theta+\dfrac{b\varsigma u}{1+au}-\varepsilon w\right), \\ {}^{FFC}D^{\zeta,\Lambda}w(t) = w(-\kappa+c\varepsilon v), \\ u(0)=g_1, v(0)=g_2, w(0)=g_3, \end{cases} \tag{1.3}$$

where u is the number of the lowest trophic species or prey, v is the number of the middle trophic level species or first predator, and w is the number of the highest trophic level species or second predator. The parameters ξ, K, ς, c, a, θ, κ, b, and ε are defined in Table 1.

The proposed operator blends non-local memory effects with the scaling behavior inherent in fractal structures, offering a more biologically consistent representation of ecological dynamics. For more about fractal-fractional calculus and its applications, please refer to [26–30].

We mention that all parameters given in Table 1 are dimensionless, scaled following standard practice to reflect interaction strengths rather than absolute population sizes.

Table 1. Description of model parameters.

Parameters	Definition	Value	Reference
ξ	It is the intrinsic growth rate of the prey.	0.5	[31]
K	It is the carrying capacity of the prey.	1.2	[32]
ς	It is the predation rate of the first predator on the prey.	1	[32]
a	It is the half saturation constant for the Holling-type predation.	1	Assumed
ε	It is the second predator's predation rate on the first predator.	1.80	Assumed
θ	It is the mortality rate of the first predator.	0.3	[33]
κ	It is the rate of mortality of the secondary predator.	0.3	[33]
b	The efficiency with which the first predator utilizes prey resources.	0.9	[32]
c	The efficiency with which the second predator utilizes prey resources.	0.8	[34]

The concept of existence results plays a crucial role in mathematical research, mainly focusing on differential equations (DEs) and the study of complex systems. This theory serves as the foundation for determining whether a given system of DEs possesses a solution, thereby enabling further analysis. Additionally, the uniqueness theorem ensures that the obtained solution is distinct. Stability analysis, on the other hand, is a highly specialized and significant area of research. It facilitates significant advancements in the study of linear and nonlinear systems, as well as in optimization and approximation theories. For several results on fixed points and stability, references can be found in [35–40].

The equilibrium points $E_1(\hat{u}, \hat{v}, \hat{w})$, $E_2(\hat{u}, \hat{v}, \hat{w})$, $E_3(\hat{u}, \hat{v}, \hat{w})$, and $E_4(\hat{u}, \hat{v}, \hat{w})$ of the model specifically named as trivial equilibrium, prey-only equilibrium, prey-predator equilibrium, and coexistence equilibrium, respectively, are derived by setting

$$u' = 0 \Rightarrow u\left[\xi\left(1 - \frac{u}{K}\right) - \frac{\varsigma v}{1 + au}\right] = 0, \tag{1.4}$$

$$v' = 0 \Rightarrow v\left(-\theta + \frac{b\varsigma u}{1 + au} - \varepsilon w\right) = 0, \tag{1.5}$$

$$w' = 0 \Rightarrow w(-\kappa + c\varepsilon v) = 0. \tag{1.6}$$

Solving these equations for u, v, and w, we obtain the following equilibrium points:

$$E_1(\hat{u}, \hat{v}, \hat{w}) = (0, 0, 0), \tag{1.7}$$

$$E_2(\hat{u}, \hat{v}, \hat{w}) = (K, 0, 0), \tag{1.8}$$

$$E_3(\hat{u}, \hat{v}, \hat{w}) = \left(\frac{\theta}{b\varsigma - \theta a}, \frac{\xi b\left[K(b\varsigma - \theta a) - \theta\right]}{K(b\varsigma - \theta a)^2}, 0\right), \tag{1.9}$$

$$E_4(\hat{u}, \hat{v}, \hat{w}) = \left(\frac{K\xi c\varepsilon}{(\xi c\varepsilon + \varsigma\kappa)}, \frac{\kappa}{c\varepsilon}, \left(\frac{1}{\varepsilon}\right)\left(-\theta + \frac{b\varsigma K}{(1 + aK)}\right) - \frac{\left(b\varsigma^2 K\kappa\right)}{\xi c\varepsilon(1 + au)(1 + aK)}\right). \tag{1.10}$$

To investigate the stability of the trivial equilibrium, we need to compute the Jacobian matrix of the system at this equilibrium. That is:

$$J = \begin{pmatrix} \frac{\partial \Phi_1}{\partial u} & \frac{\partial \Phi_1}{\partial v} & \frac{\partial \Phi_1}{\partial w} \\ \frac{\partial \Phi_2}{\partial u} & \frac{\partial \Phi_2}{\partial v} & \frac{\partial \Phi_2}{\partial w} \\ \frac{\partial \Phi_3}{\partial u} & \frac{\partial \Phi_3}{\partial v} & \frac{\partial \Phi_3}{\partial w} \end{pmatrix}, \tag{1.11}$$

where Φ_1, Φ_2, and Φ_3 are the right-hand sides of the model equations. Deriving the matrix J in (1.11) at the trivial equilibrium $(0, 0, 0)$, we obtain:

$$J = \begin{pmatrix} \xi & 0 & 0 \\ 0 & -\theta & 0 \\ 0 & 0 & -\kappa \end{pmatrix}. \tag{1.12}$$

The eigenvalues are:

$$\lambda_1 = \xi, \tag{1.13}$$
$$\lambda_2 = -\theta, \tag{1.14}$$
$$\lambda_3 = -\kappa. \tag{1.15}$$

For stability, we need $\lambda_1 < 0 \Rightarrow \xi < 0$, which is not possible because ξ is the intrinsic growth rate of the prey. Similarly, $\lambda_2 > 0 \Rightarrow \theta < 0$, which is also not possible because θ is the mortality rate. Likewise, $\lambda_3 > 0 \Rightarrow \kappa < 0$, which is also not possible because κ is the mortality rate.

Since one of the eigenvalues (λ_1) is positive, the trivial equilibrium is unstable, causing the system to move away, leading to population growth or decline.

Prey-only equilibrium $(K, 0, 0)$: The prey-only equilibrium $(K, 0, 0)$ is found by setting $v = 0$ and $w = 0$ in the model (1.2) equations. As a first step, we obtain:

$$u' = u\left[\xi\left(1 - \frac{u}{K}\right)\right]. \tag{1.16}$$

Solving (1.16) for u, we obtain the prey-only equilibrium as $E_2(\hat{u}, \hat{v}, \hat{w}) = (K, 0, 0)$. Analyzing the stability of the prey-only equilibrium requires calculation of the matrix (1.11) of the system at this equilibrium as below:

$$J = \begin{pmatrix} -\xi & -\frac{\varsigma}{1+aK} & 0 \\ 0 & \frac{b\varsigma}{1+aK} - \theta & 0 \\ 0 & 0 & -\kappa + c\varepsilon(\frac{b\varsigma}{1+aK}) \end{pmatrix}. \tag{1.17}$$

We proceed to examine the eigenvalues of the concerned matrix (1.17). The eigenvalues are:

$$\lambda_4 = -\xi, \tag{1.18}$$
$$\lambda_5 = \frac{b\varsigma}{1+aK} - \theta, \tag{1.19}$$
$$\lambda_6 = -\kappa + c\varepsilon(\frac{b\varsigma}{1+aK}). \tag{1.20}$$

For the stability of the model, we need all the eigenvalues to be negative. Obviously $\lambda_4 = -\xi < 0$. The values of λ_5, λ_6 depend on the specific values of the parameters involved in $\frac{b\varsigma}{1+aK} - \theta$ and $-\kappa + c\varepsilon(\frac{b\varsigma}{1+aK})$, respectively.

The prey-predator equilibrium $E_3(\hat{u}, \hat{v}, \hat{w})$: The prey-predator equilibrium is determined by setting $w = 0$ in the model (1.2) equations and solving for $u = 0$ and $v = 0$. For equilibrium, we set the first two equations equal to zero. That is

$$u\left[\xi\left(1 - \frac{u}{K}\right) - \frac{\varsigma v}{1+au}\right] = 0, \tag{1.21}$$

$$v\Big(-\theta+\frac{b\varsigma u}{1+au}-\varepsilon w\Big)=0. \tag{1.22}$$

Solving for u and v, we find that $(u,v,w)=E_3(\hat{u},\hat{v},0)$, where u and v satisfy the equations:

$$\xi\Big(1-\frac{\hat{u}}{K}\Big)-\frac{\varsigma\hat{v}}{1+a\hat{u}}=0, \tag{1.23}$$

$$-\frac{b\varsigma\hat{u}}{1+a\hat{u}}+\theta=0. \tag{1.24}$$

Similarly, analyzing the stability of the prey-predator equilibrium requires calculation of the matrix (1.11) of the system at this equilibrium. Then, as above, we can discuss its stability by looking into the corresponding eigenvalues. Similarly, we can discuss the stability of coexistence equilibrium $E_4(\hat{u},\hat{v},\hat{w})$. Also one may see the article [24], where the stability of $E_3(\hat{u},\hat{v},\hat{w})$ and $E_4(\hat{u},\hat{v},\hat{w})$ have been discussed in detail.

The system of Eq (1.1) can be represented as

$${}^{FFC}D^{\zeta,\Lambda}\xi(t)=\begin{cases}\Theta(t,\xi(t)),\\ \xi(0)=\xi_0,\quad t\in[0,T]=:\Upsilon,\end{cases} \tag{1.25}$$

where the vector $\xi(t)=(u,v,w)$, and Θ is expressed as

$$\Theta(t,\xi(t))=\begin{bmatrix}\Lambda t^{\Lambda-1}\Phi_1(t,u,v,w)\\ \Lambda t^{\Lambda-1}\Phi_2(t,u,v,w)\\ \Lambda t^{\Lambda-1}\Phi_3(t,u,v,w)\end{bmatrix}, \tag{1.26}$$

$$\xi(t)=\begin{bmatrix}\Phi_1\\ \Phi_2\\ \Phi_3\end{bmatrix}=\begin{bmatrix}u(t)\\ v(t)\\ w(t)\end{bmatrix}=\begin{bmatrix}u\Big[\xi\Big(1-\frac{u}{K}\Big)-\frac{\varsigma v}{1+au}\Big]\\ v\Big(-\theta+\frac{b\varsigma u}{1+au}-\varepsilon w\Big)\\ w(-\kappa+c\varepsilon v)\end{bmatrix},\ \xi_0=\begin{bmatrix}g_1\\ g_2\\ g_3\end{bmatrix}. \tag{1.27}$$

From (1.26) and (1.27), problem (1.25) follows as

$$\begin{cases}{}^{FFC}D^{\zeta,\Lambda}u(t)=\Lambda t^{\Lambda-1}\Phi_1(t,u,v,w),\\ {}^{FFC}D^{\zeta,\Lambda}v(t)=\Lambda t^{\Lambda-1}\Phi_2(t,u,v,w),\\ {}^{FFC}D^{\zeta,\Lambda}w(t)=\Lambda t^{\Lambda-1}\Phi_3(t,u,v,w);\end{cases} \tag{1.28}$$

where $\Phi_1,\Phi_2,\Phi_3:\Upsilon\times\mathbf{R}^3\to\mathbf{R}$ are continuous. We can express (1.28) as

$${}^{FFC}D^{\zeta,\Lambda}\mathbb{X}(t)=\begin{cases}\Lambda t^{\Lambda-1}\Phi_1(t,\mathbb{X}(t)),\\ \Lambda t^{\Lambda-1}\Phi_2(t,\mathbb{X}(t)),\\ \Lambda t^{\Lambda-1}\Phi_3(t,\mathbb{X}(t)),\\ \mathbb{X}(0)=\mathbb{X}_0,\quad t\in\Upsilon.\end{cases} \tag{1.29}$$

This manuscript is organized into several key sections. Following the introduction, Section 2 lays the foundation with essential definitions and preliminary findings. Section 3 delves into the

existence and stability of solutions, providing a critical framework for analysis. A numerical scheme is demonstrated in Section 4, giving the computation of numerical solutions. These solutions are then simulated and visualized in Section 5, yielding critical insights into the underlying dynamics. Section 6 presents a detailed discussion and interpretation of the simulated results. Finally, Section 7 synthesizing the major findings into a cohesive narrative.

2. Materials and methods

The sup norm $\|.\|_{\Upsilon}$ is defined as follows:

$$\|g(t)\|_{\Upsilon} = \sup_{\Upsilon} \|g(t)\|, \quad g(t) \in C(\Upsilon, \mathbf{R}^3). \tag{2.1}$$

Here $C(\Upsilon, \mathbf{R}^3) := \mathbb{I}$ is forming a Banach space with the norm $\|.\|_{\Upsilon}$.

Definition 2.1. [26] Assume y is a continuous mapping that is fractal differentiable on Υ. In Riemann-Liouville (R-L) framework, the fractal-fractional integral is expressed as

$${}^{FF}I^{\zeta,\Lambda}y(t) = \frac{\Lambda}{\Gamma(\zeta)} \int_a^t \theta^{\Lambda-1}(t-\theta)^{\zeta-1} y(\theta) d\theta. \tag{2.2}$$

Definition 2.2. [26] For functions y belonging to the space $C[0, T]$, the FF-Caputo derivative of order ζ associated with fractal dimension Λ is expressed as

$${}^{FFC}D^{\zeta,\Lambda}y(t) = \frac{1}{\Gamma(1-\zeta)} \int_a^t (t-\theta)^{-\zeta} \frac{d}{dt^{\Lambda}} y(\theta) d\theta, \quad 0 < \zeta, \Lambda \leq 1. \tag{2.3}$$

Definition 2.3. The ABM method for solving ordinary DEs is given by

$$s_{n+1} = s_n + h \sum_{i=1}^{r} m_i f(\tau_n + ih, s_n + ih).$$

This formula involves the computed (approximate) solution s_n, step size h, ODE $f(s, \tau)$, and coefficients m_i.

Lemma 2.1. *The solution of*

$$\begin{aligned} {}^{FFC}D^{\zeta,\Lambda}\mathbb{X}(t) &= h(t), \quad \zeta \in (0, 1], \\ \mathbb{X}(0) &= \mathbb{X}_0, \end{aligned}$$

is given by

$$\mathbb{X}(t) = \mathbb{X}_0 + \frac{\Lambda}{\Gamma(\zeta)} \int_0^t x^{\Lambda-1}(t-x)^{\zeta-1} h(x) dx, \quad t \in \Upsilon. \tag{2.4}$$

Proof. We omit the proof as it is straightforward. □

Corollary 2.1. *From Lemma 2.1, it follows that the solution of* (1.25) *is equivalent to the integral equation provided by*

$$\mathbb{X}(t) = \mathbb{X}_0 + \frac{\Lambda}{\Gamma(\zeta)} \int_0^t x^{\Lambda-1}(t-x)^{\zeta-1} \Psi(x, \mathbb{X}(x)) dx, \quad t \in \Upsilon. \tag{2.5}$$

3. Results

3.1. Existence of solutions

In this section, we investigate whether the system under consideration admits a solution. To achieve this, we employ the fixed-point approach.

Prior to deriving our main results, we define the operator $F : \mathbf{I} \to \mathbf{I}$ as follows:

$$F(\mathbb{X}) = \mathbb{X}_0 + \frac{\Lambda}{\Gamma(\zeta)} \int_0^t x^{\Lambda-1}(t-x)^{\zeta-1}\Psi(x, \mathbb{X}(x))dx, \quad t \in \Upsilon. \tag{3.1}$$

Also we need to assume that

(D_1) For $\mathbb{X}, \bar{\mathbb{X}} \in \mathbf{I}$, there is $\mathbb{K}_\Psi > 0$, fulfilling

$$|\Psi(t, \mathbb{X}(t)) - \Psi(t, \bar{\mathbb{X}}(t))| \leq \mathbb{K}_\Psi |\mathbb{X}(t) - \bar{\mathbb{X}}(t)|.$$

(D_2) $\mathbb{N}_0, \mathbb{N}_1 > 0$ are holding the inequality

$$|\Psi(t, \mathbb{X}(t))| \leq \mathbb{N}_0 + \mathbb{N}_1 |\mathbb{X}(t)|.$$

Theorem 3.1. *Suppose that condition* (D_1) *is satisfied and that* $\ell\mathbb{K}_\Psi\beta(\zeta, \Lambda) < 1$. *Then, the problem* (1.25) *possesses a unique solution.*

Proof. On the interval Υ, we consider

$$\begin{aligned} |F(\mathbb{X})(t) - F(\overline{\mathbb{X}})(t)| &\leq \frac{\Lambda}{\Gamma(\zeta)} \int_0^t x^{\Lambda-1}(t-x)^{\zeta-1}|\Psi(x, \mathbb{X}(x)) - \Psi(x, \overline{\mathbb{X}}(x))|dx \\ &\leq \frac{\Lambda\mathbb{K}_\Psi}{\Gamma(\zeta)} \int_0^t x^{\Lambda-1}(t-x)^{\zeta-1}\|\mathbb{X} - \bar{\mathbb{X}}\|dx. \end{aligned} \tag{3.2}$$

Consider the integral $\int_0^t x^{\Lambda-1}(t-x)^{\zeta-1}dx$. Let $x = ty$. This implies that $dx = tdy$. If $x = 0$, then $y = 0$ and if $x = t$, then $y = 1$. This gives

$$\begin{aligned} \int_0^t x^{\Lambda-1}(t-x)^{\zeta-1}dx &= t^{\Lambda+\zeta-1}\int_0^1 y^{\Lambda-1}(1-y)^{\zeta-1}dy \leq t^{\Lambda+\zeta-1}\int_0^1 y^{\Lambda-1}(1-y)^{\zeta-1}dy \\ &= t^{\Lambda+\zeta-1}\beta(\zeta, \Lambda). \end{aligned} \tag{3.3}$$

In the above equation $\beta(\zeta, \Lambda)$ represents the beta function. It follows from (3.2) that

$$\|F(\mathbb{X}) - F(\overline{\mathbb{X}})\| \leq \frac{\Lambda\mathbb{K}_\Psi T^{\Lambda+\zeta-1}}{\Gamma(\zeta)}\beta(\zeta, \Lambda)\|\mathbb{X} - \bar{\mathbb{X}}\|. \tag{3.4}$$

Lets denote $\frac{\Lambda T^{\Lambda+\zeta-1}}{\Gamma(\zeta)}$ by ℓ. Then

$$\begin{aligned} \|F(\mathbb{X}) - F(\overline{\mathbb{X}})\| &\leq \ell\mathbb{K}_\Psi \int_0^1 z^{\Lambda-1}(1-z)^{\zeta-1}\|\mathbb{X} - \bar{\mathbb{X}}\|dz \\ &\leq \ell\mathbb{K}_\Psi\beta(\zeta, \Lambda)\|\mathbb{X} - \bar{\mathbb{X}}\|. \end{aligned} \tag{3.5}$$

Now since $\ell\mathbb{K}_\Psi\beta(\zeta, \Lambda) < 1$, therefore, from (3.5), we deduced that the operator F has a unique fixed point. □

Theorem 3.2. *Assuming the condition* (D_1) *holds, then problem* (1.25) *possesses one or more solutions.*

Proof. To establish this result, we recall the operator F defined by

$$F = \mathbb{X}(0) + \frac{\Lambda}{\Gamma(\zeta)} \int_0^t x^{\Lambda-1}(t-x)^{\zeta-1}\Psi(x, \mathbb{X}(x))dx, \quad if\ t \in \Upsilon. \tag{3.6}$$

We choose a closed ball $\mho_\Omega = \{\mathbb{X} \in \mathbf{I} : \|\mathbb{X}\| \leq \Omega\}$ which satisfies

$$\Omega \geq \max\left\{ \|\mathbb{X}(0)\| + \frac{\Lambda T^{\Lambda+\zeta-1}\beta(\zeta,\Lambda)}{\Gamma(\zeta)}(N_0 + \mathbb{N}_1\Omega)\right\}.$$

We will now provide a step-by-step proof to establish this result.

Step 1: $F\mathbb{X}(t) \in \mho_\Omega$. For $t \in \Upsilon$, $\mathbb{X} \in \mho_\Omega$, we have

$$\begin{aligned} |F\mathbb{X}(t)| &= \left| \mathbb{X}(0) + \frac{\Lambda}{\Gamma(\zeta)} \int_0^t x^{\Lambda-1}(t-x)^{\zeta-1}\Psi(x, \mathbb{X}(x))dx \right| \\ &\leq |\mathbb{X}(0)| + \frac{\Lambda}{\Gamma(\zeta)} \int_0^t x^{\Lambda-1}(t-x)^{\zeta-1} \left|\Psi(x, \mathbb{X}(x))\right| dx \\ &\leq |\mathbb{X}(0)| + \frac{\Lambda}{\Gamma(\zeta)} \int_0^t x^{\Lambda-1}(t-x)^{\zeta-1} \left(\mathbb{N}_0 + \mathbb{N}_1|\mathbb{X}(t)|\right) dx. \end{aligned} \tag{3.7}$$

Applying the transformation as used in (3.3),

$$\begin{aligned} \int_0^t x^{\Lambda-1}(t-x)^{\zeta-1}dx &\leq t^{\Lambda+\zeta-1} \int_0^1 y^{\Lambda-1}(1-y)^{\zeta-1}dy \\ &= t^{\Lambda+\zeta-1}\beta(\zeta,\Lambda), \end{aligned}$$

and from (3.7), we have

$$|F\mathbb{X}(t)| \leq |\mathbb{X}(0)| + \frac{\Lambda t^{\Lambda+\zeta-1}\mathbb{N}_0}{\Gamma(\zeta)}\beta(\zeta,\Lambda) + \frac{\Lambda t^{\Lambda+\zeta-1}\mathbb{N}_1\Omega}{\Gamma(\zeta)}\beta(\zeta,\Lambda) \leq \Omega. \tag{3.8}$$

This implies

$$\|F\mathbb{X}\| \leq \|\mathbb{X}(0)\| + \frac{\Lambda T^{\Lambda+\zeta-1}\beta(\zeta,\Lambda)}{\Gamma(\zeta)}(N_0 + \mathbb{N}_1\Omega) \leq \Omega. \tag{3.9}$$

Step 2: We establish the relative compactness of F. Since $\Psi(t, \mathbb{X}(t))$ is continuous, it follows that F is continuous too.

We demonstrate that F is uniformly bounded on the given closed ball $\mho_\Omega$. We proceed as follows:

For $t \in [0, T]$, $\mathbb{X} \in \mho_\Omega$.

$$|F\mathbb{X}(t)| \quad \leq \quad |\mathbb{X}(0)| + \sup_{t\in(0,T]} \frac{\Lambda}{\Gamma(\zeta)} \int_0^t x^{\Lambda-1}(t-x)^{\zeta-1} \left|\Psi(x, \mathbb{X}(x))\right| dx.$$

Using assumption (D_2) and the transformation given in (3.3), we have

$$|F\mathbb{X}(t)| \quad \leq \quad |\mathbb{X}(0)| + \frac{\Lambda T^{\Lambda+\zeta-1}\left(\mathbb{N}_0 + \mathbb{N}_1\Omega\right)}{\Gamma(\zeta)}\beta(\zeta,\Lambda) \leq \Omega.$$

We have shown that F is uniformly bounded on $\mathfrak{V}_\Omega$. The remaining task is to prove that F is equi-continuous. Take any $t_a, t_b \in [0, T]$, with $t_a < t_b$ and $\mathbb{X} \in \mathfrak{V}_\Omega$, and we have

$$\begin{aligned} &|F\mathbb{X}(t_b) - F_2\mathbb{X}(t_a)| \\ &\leq \left|\frac{\Lambda}{\Gamma(\zeta)}\Big(\int_0^{t_b} x^{\Lambda-1}(t_b - x)^{\zeta-1}\Psi(x, \mathbb{X}(x))dx - \int_0^{t_a} x^{\Lambda-1}(t_a - x)^{\zeta-1}\Psi(x, \mathbb{X}(x))dx\Big)\right|. \end{aligned} \tag{3.10}$$

In the integral $\int_0^{t_b} x^{\Lambda-1}(t_b - x)^{\zeta-1}dx$, let $x = t_b y$. Then $dx = t_b dy$. We get $y = 0$ for $x = 0$ and $y = 1$ for $x = t_b$. The integral converts into: ${t_b}^{\Lambda+\zeta-1}\int_0^1 y^{\Lambda-1}(1-y)^{\zeta-1}dy$. Similarly, in the integral $\int_0^{t_a} x^{\Lambda-1}(t_a - x)^{\zeta-1}\Psi(x, \mathbb{X}(x))dx$, by taking $x = t_a y$, the integral gets the form ${t_a}^{\Lambda+\zeta-1}\int_0^1 y^{\Lambda-1}(1-y)^{\zeta-1}dy$. Applying the transformed results and assumption (D_2), (3.10) becomes

$$\begin{aligned} &|F\mathbb{X}(t_b) - F\mathbb{X}(t_a)| \\ &\leq \left|\frac{\Lambda(\mathbb{N}_0 + \mathbb{N}_1\Omega)}{\Gamma(\zeta)}\Big({t_b}^{\Lambda+\zeta-1}\int_0^1 y^{\Lambda-1}(1-y)^{\zeta-1}dy - {t_a}^{\Lambda+\zeta-1}\int_0^1 y^{\Lambda-1}(1-y)^{\zeta-1}dy\Big)\right| \\ &\to 0 \text{ as } t_a \to t_b. \end{aligned} \tag{3.11}$$

This establishes the equi-continuity of F. By the Arzelá-Ascoli theorem and the preceding steps, we have shown that F is relatively compact, and hence has complete continuity. Therefore, Schaefer's fixed-point theorem guarantees the existence of one or more solutions to the problem (1.25) under consideration. □

3.2. Stability results

In this section, we employ the H-U approach to establish stability conditions for the problem under consideration.

Definition 3.1. The model (1.25) is H-U stable if there exists a real number $\mathbb{C} = \max\{\mathbb{C}_1, \mathbb{C}_2, \mathbb{C}_3\} > 0$ such that for each $\epsilon = \max\{\epsilon_1, \epsilon_2, \epsilon_3\} > 0$, there is a solution $\overline{\mathbb{X}} \in \mathbf{I}$ of (3.12),

$$\left|{}^{FFC}D^{\zeta,\Lambda}\overline{\mathbb{X}}(t) - \Theta(t, \overline{\mathbb{X}}(t))\right| \leq \epsilon, t \in J, \tag{3.12}$$

associated with the unique solution $\mathbb{X} \in \mathbf{I}$ of the model (1.25), such that

$$\left\|\overline{\mathbb{X}} - \mathbb{X}\right\| \leq \mathbb{C}\epsilon, \qquad t \in J,$$

where

$$\overline{\mathbb{X}}(t) = \begin{bmatrix} \overline{u}(t) \\ \overline{v}(t) \\ \overline{w}(t) \end{bmatrix} = \begin{bmatrix} \overline{u}\Big[\Lambda\Big(1 - \dfrac{\overline{u}}{K}\Big) - \dfrac{\varsigma\overline{v}}{1 + a\overline{u}}\Big] \\ \overline{v}\Big(-\theta + \dfrac{b\varsigma\overline{u}}{1 + a\overline{u}} - \varepsilon\overline{w}\Big) \\ \overline{w}(-\kappa + c\varepsilon\overline{v}) \end{bmatrix},$$

$$\Theta(t, \overline{\mathbb{X}}(t)) = \begin{bmatrix} \Lambda t^{\Lambda-1}\overline{\Phi}_1(t, \overline{u}, \overline{v}, \overline{w}) \\ \Lambda t^{\Lambda-1}\overline{\Phi}_2(t, \overline{u}, \overline{v}, \overline{w}) \\ \Lambda t^{\Lambda-1}\overline{\Phi}_3(t, \overline{u}, \overline{v}, \overline{w}) \end{bmatrix}, \overline{\mathbb{X}}_0 = \begin{bmatrix} \overline{g}_1 \\ \overline{g}_2 \\ \overline{g}_3 \end{bmatrix}.$$

Remark 3.1. The following inequality holds for function $\overline{\mathbb{X}} \in \mathbf{I}$.

$$\left|{}^{FFC}D^{\zeta,\Lambda}\overline{\mathbb{X}}(t) - \Theta(t, \overline{\mathbb{X}}(t))\right| \leq \epsilon, t \in J,$$

iff one can find a small perturbation $\alpha \in \mathbf{I}$ satisfying

(*i*) $|\alpha(t)| \leq \epsilon, t \in J$;
(*ii*) ${}^{FFC}D^{\zeta,\Lambda}\overline{\mathbb{X}}(t) = \Theta(t, \overline{\mathbb{X}}(t)) + \alpha(t), t \in J,$

where $\alpha(t) = (t, \alpha_1(t), \alpha_2(t), \alpha_3(t))$.

From Remark 3.1, it follows that we have a problem involving a small perturbation function $\alpha(t)$, given as

$${}^{FFC}D^{\zeta,\Lambda}\overline{\mathbb{X}}(t) = \begin{cases} \Theta(t, \overline{\mathbb{X}}(t)) + \alpha(t), \\ \overline{\mathbb{X}}(0) = \overline{\mathbb{X}}_0, \quad t \in \Upsilon. \end{cases} \tag{3.13}$$

Lemma 3.1. *Problem* (3.13) *with the perturbation function* $\alpha(t)$ *has a solution given as*

$$\overline{\mathbb{X}}(t) = \overline{\mathbb{X}}_0 + \frac{\Lambda}{\Gamma(\zeta)}\int_0^t x^{\Lambda-1}(t-x)^{\zeta-1}(\Theta(x, \overline{\mathbb{X}}(x)) + \alpha(x))dx, \quad t \in \Upsilon. \tag{3.14}$$

Theorem 3.3. *Assuming* (D_1) *holds and* $\ell\mathbb{K}_\Psi\beta(\zeta, \Lambda) < 1$, *then in the sense of H-U stability, problem* (1.25) *is stable.*

Proof. Considering any solution $\overline{\mathbb{X}} \in \mathbf{I}$ of inequality (3.12) and the unique solution $\mathbb{X} \in \mathbf{I}$ of model (1.25), we examine the following:

$$\begin{aligned} |\overline{\mathbb{X}}(t) - \mathbb{X}(t)| &\leq \frac{\Lambda}{\Gamma(\zeta)}\int_0^t x^{\Lambda-1}(t-x)^{\zeta-1}|\Theta(x, \overline{\mathbb{X}}(x)) - \Theta(x, \mathbb{X}(x))|dx \\ &\quad + \frac{\Lambda}{\Gamma(\zeta)}\int_0^t x^{\Lambda-1}(t-x)^{\zeta-1}|\alpha(x)|dx \\ &\leq \frac{\Lambda\mathbb{K}_\Theta}{\Gamma(\zeta)}\int_0^t x^{\Lambda-1}(t-x)^{\zeta-1}|\overline{\mathbb{X}}(x) - \mathbb{X}(x)|dx \\ &\quad + \frac{\Lambda\epsilon}{\Gamma(\zeta)}\int_0^t x^{\Lambda-1}(t-x)^{\zeta-1}dx. \end{aligned} \tag{3.15}$$

As in Theorem 3.1, take the integral $\int_0^t x^{\Lambda-1}(t-x)^{\zeta-1}dx$. Let $x = ty$. That implies $dx = tdy$. We get $y = 0$ for $x = 0$ and $y = 1$ for $x = t$. Substituting the values, we have

$$\int_0^t x^{\Lambda-1}(t-x)^{\zeta-1}dx = t^{\Lambda+\zeta-1}\int_0^1 y^{\Lambda-1}(1-y)^{\zeta-1}dy. \tag{3.16}$$

Thus from the last inequality, we have

$$\begin{aligned} |\overline{\mathbb{X}}(t) - \mathbb{X}(t)| &\leq \frac{\Lambda\mathbb{K}_\Theta}{\Gamma(\zeta)}t^{\Lambda+\zeta-1}\int_0^1 y^{\Lambda-1}(1-y)^{\zeta-1}|\overline{\mathbb{X}}(x) - \mathbb{X}(x)|dy \\ &\quad + \frac{\Lambda\epsilon}{\Gamma(\zeta)}t^{\Lambda+\zeta-1}\int_0^1 y^{\Lambda-1}(1-y)^{\zeta-1}dy. \end{aligned} \tag{3.17}$$

Use $\int_0^1 y^{\Lambda-1}(1-y)^{\zeta-1}dy = \beta(\zeta,\Lambda)$, and we have

$$|\overline{\mathbb{X}}(t)-\mathbb{X}(t)| \leq \frac{\Lambda}{\Gamma(\zeta)}t^{\Lambda+\zeta-1}\mathbb{K}_{\Theta}\beta(\zeta,\Lambda)|\overline{\mathbb{X}}(t)-\mathbb{X}(t)| + \ell\beta(\zeta,\Lambda)\epsilon. \tag{3.18}$$

Taking the maximum and using ℓ for $\frac{\Lambda}{\Gamma(\zeta)}T^{\Lambda+\zeta-1}$, we have

$$\|\overline{\mathbb{X}}-\mathbb{X}\| \leq \frac{\ell\beta(\zeta,\Lambda)}{1-\ell\mathbb{K}_{\Theta}\beta(\zeta,\Lambda)}\epsilon. \tag{3.19}$$

Choose $\mathbb{C} > 0$ such that

$$\mathbb{C} = \frac{\ell\beta(\zeta,\Lambda)}{1-\ell\mathbb{K}_{\Theta}\beta(\zeta,\Lambda)}, \quad if\ t \in \Upsilon.$$

Hence

$$\|\overline{\mathbb{X}}-\mathbb{X}\| \leq \mathbb{C}\epsilon. \tag{3.20}$$

It follows that model (1.25) exhibits H-U stability. □

4. Numerical schemes

In this part of the paper, we develop a numerical approach for the proposed tri-trophic food web model by employing the ABM along with Lagrangian piecewise interpolation [41]. This technique has been widely utilized for approximating solutions to nonlinear fractal-fractional order problems and has found significant applications in epidemic modeling (refer to [33, 34]).

The integral formulation of the considered model at $t = t_{r+1}$ is presented as

$$\begin{cases} u^{r+1} = u(0) + \frac{\Lambda}{\Gamma(\zeta)}\int_0^{t_{r+1}} x^{\Lambda-1}(t_{r+1}-x)^{\zeta-1}\Phi_1(x,u,v,w)dx, & t_{r+1} \in \Upsilon, \\ v^{r+1} = v(0) + \frac{\Lambda}{\Gamma(\zeta)}\int_0^{t_{r+1}} x^{\Lambda-1}(t_{r+1}-x)^{\zeta-1}\Phi_1(x,u,v,w)dx, & t_{r+1} \in \Upsilon, \\ w^{r+1} = w(0) + \frac{\Lambda}{\Gamma(\zeta)}\int_0^{t_{r+1}} x^{\Lambda-1}(t_{r+1}-x)^{\zeta-1}\Phi_1(x,u,v,w)dx, & t_{r+1} \in \Upsilon. \end{cases} \tag{4.1}$$

Approximating the system of Eq (4.1) yields

$$\begin{cases} u^{r+1} = u(0) + \frac{\Lambda}{\Gamma(\zeta)}\sum_{\vartheta=0}^{r}\int_{t_\vartheta}^{t_{r+1}} x^{\Lambda-1}(t_{r+1}-x)^{\zeta-1}\Phi_1(x,u,v,w)dx, & t_{r+1} \in \Upsilon, \\ v^{r+1} = v(0) + \frac{\Lambda}{\Gamma(\zeta)}\sum_{\vartheta=0}^{r}\int_{t_\vartheta}^{t_{r+1}} x^{\Lambda-1}(t_{r+1}-x)^{\zeta-1}\Phi_1(x,u,v,w)dx, & t_{r+1} \in \Upsilon, \\ w^{r+1} = w(0) + \frac{\Lambda}{\Gamma(\zeta)}\sum_{\vartheta=0}^{r}\int_{t_\vartheta}^{t_{r+1}} x^{\Lambda-1}(t_{r+1}-x)^{\zeta-1}\Phi_1(x,u,v,w)dx, & t_{r+1} \in \Upsilon. \end{cases} \tag{4.2}$$

To approximate the kernels within the integrals, we employ Lagrangian polynomial piecewise interpolation on the interval $[t_r, t_{r+1}]$ as given by

$$\begin{cases} \mathbb{W}_r(x) = \frac{x-t_{r-1}}{t_r-t_{r-1}}t_r^{\Lambda-1}\Phi_1(t^r,u^r,v^r,w^r) - \frac{x-t_r}{t_r-t_{r-1}}t_{r-1}^{\Lambda-1}\Phi_1(t^{r-1},u^{r-1},v^{r-1},w^{r-1}), \\ \mathbb{Y}_r(x) = \frac{x-t_{r-1}}{t_r-t_{r-1}}t_r^{\Lambda-1}\Phi_2(t^r,u^r,v^r,w^r) - \frac{x-t_r}{t_r-t_{r-1}}t_{r-1}^{\Lambda-1}\Phi_2(t^{r-1},u^{r-1},v^{r-1},w^{r-1}), \\ \mathbb{Z}_r(x) = \frac{x-t_{r-1}}{t_r-t_{r-1}}t_r^{\Lambda-1}\Phi_3(t^r,u^r,v^r,w^r) - \frac{x-t_r}{t_r-t_{r-1}}t_{r-1}^{\Lambda-1}\Phi_3(t^{r-1},u^{r-1},v^{r-1},w^{r-1}). \end{cases} \tag{4.3}$$

Using these approximations in system (4.2), we obtain

$$\begin{cases} u^{r+1} = u(0) + \frac{\Lambda}{\Gamma(\zeta)} \sum_{\vartheta=0}^{r} \int_{t_\vartheta}^{t_{r+1}} x^{\Lambda-1}(t_{r+1}-x)^{\zeta-1}\mathbb{W}_r(x)dx, \quad t_{r+1} \in \Upsilon, \\ v^{r+1} = v(0) + \frac{\Lambda}{\Gamma(\zeta)} \sum_{\vartheta=0}^{r} \int_{t_\vartheta}^{t_{r+1}} x^{\Lambda-1}(t_{r+1}-x)^{\zeta-1}\mathbb{Y}_r(x)dx, \quad t_{r+1} \in \Upsilon, \\ w^{r+1} = w(0) + \frac{\Lambda}{\Gamma(\zeta)} \sum_{\vartheta=0}^{r} \int_{t_\vartheta}^{t_{r+1}} x^{\Lambda-1}(t_{r+1}-x)^{\zeta-1}\mathbb{Z}_r(x)dx, \quad t_{r+1} \in \Upsilon. \end{cases} \tag{4.4}$$

Piecewise interpolation using a Lagrangian polynomial, followed by integration, gives the scheme for the numerical solution to the considered problem as

$$\begin{cases} u^{r+1} = u(0) + \frac{\Lambda h^\zeta}{\Gamma(\zeta+2)} \sum_{\vartheta=1}^{r} \Big[t_\vartheta^{\Lambda-1}\Phi_1(t_\vartheta, u^\vartheta, v^\vartheta, w^\vartheta)\Big((r+1-\vartheta)^\zeta(r-\vartheta+2+\zeta) \\ \quad - (r-\vartheta)^\zeta(r-\vartheta+2+2\zeta)\Big) - t_{\vartheta-1}^{\Lambda-1}\Phi_1(t_{\vartheta-1}, u^{\vartheta-1}, v^{\vartheta-1}, w^{\vartheta-1}) \\ \quad \times \Big((r-\vartheta+1)^{\zeta-1} - (r-\vartheta)^\zeta(r-\vartheta+1+\zeta)\Big)\Big], \quad t_\vartheta, t_{\vartheta-1} \in \Upsilon; \\ v^{r+1} = v(0) + \frac{\Lambda h^\zeta}{\Gamma(\zeta+2)} \sum_{\vartheta=1}^{r} \Big[t_\vartheta^{\Lambda-1}\Phi_2(t_\vartheta, u^\vartheta, v^\vartheta, w^\vartheta)\Big((r+1-\vartheta)^\zeta(r-\vartheta+2+\zeta) \\ \quad - (r-\vartheta)^\zeta(r-\vartheta+2+2\zeta)\Big) - t_{\vartheta-1}^{\Lambda-1}\Phi_2(t_{\vartheta-1}, u^{\vartheta-1}, v^{\vartheta-1}, w^{\vartheta-1}) \\ \quad \times \Big((r-\vartheta+1)^{\zeta-1} - (r-\vartheta)^\zeta(r-\vartheta+1+\zeta)\Big)\Big], \quad t_\vartheta, t_{\vartheta-1} \in \Upsilon; \\ w^{r+1} = w(0) + \frac{\Lambda h^\zeta}{\Gamma(\zeta+2)} \sum_{\vartheta=1}^{r} \Big[t_\vartheta^{\Lambda-1}\Phi_3(t_\vartheta, u^\vartheta, v^\vartheta, w^\vartheta)\Big((r+1-\vartheta)^\zeta(r-\vartheta+2+\zeta) \\ \quad - (r-\vartheta)^\zeta(r-\vartheta+2+2\zeta)\Big) - t_{\vartheta-1}^{\Lambda-1}\Phi_3(t_{\vartheta-1}, u^{\vartheta-1}, v^{\vartheta-1}, w^{\vartheta-1}) \\ \quad \times \Big((r-\vartheta+1)^{\zeta-1} - (r-\vartheta)^\zeta(r-\vartheta+1+\zeta)\Big)\Big], \quad t_\vartheta, t_{\vartheta-1} \in \Upsilon. \end{cases} \tag{4.5}$$

5. Graphical interpretation of results through simulations

Here we proceed by simulating the results to graphically interpret them (Figures 1–8) and to validate our approach. We use MATLAB for this purpose.

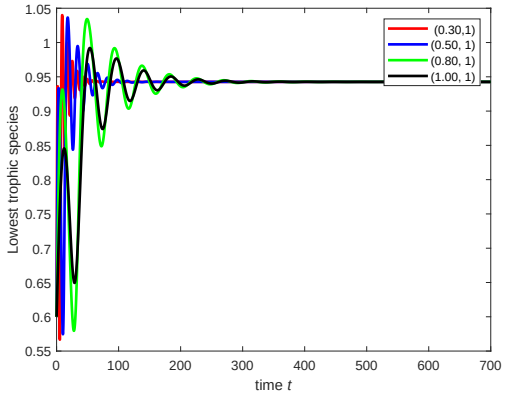

Figure 1. Impact of fractional order on the population dynamics of the lowest trophic species in time t.

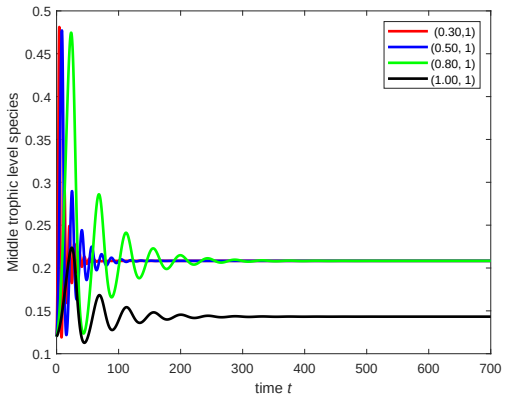

Figure 2. Impact of fractional order on the population dynamics of the middle trophic level species in time t.

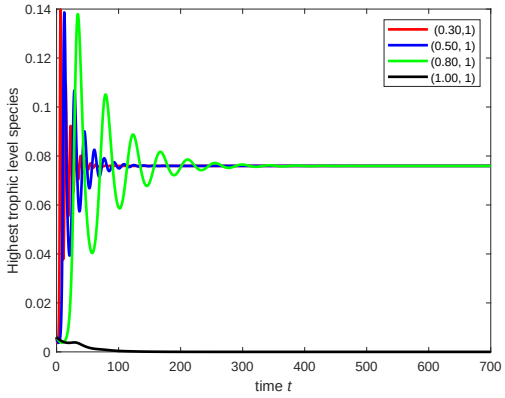

Figure 3. Impact of the fractional order on the population dynamics of the highest trophic level species in time t.

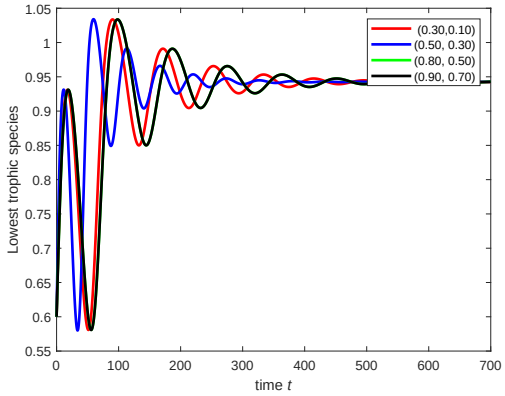

Figure 4. Impact of the fractal dimension on the population dynamics of the lowest trophic level species in time t.

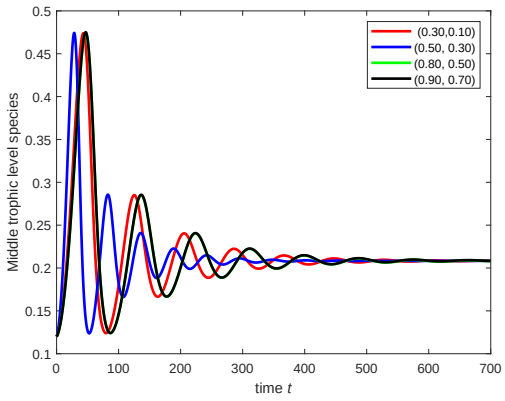

Figure 5. Impact of fractal dimension on the population dynamics of the middle trophic level species in time t.

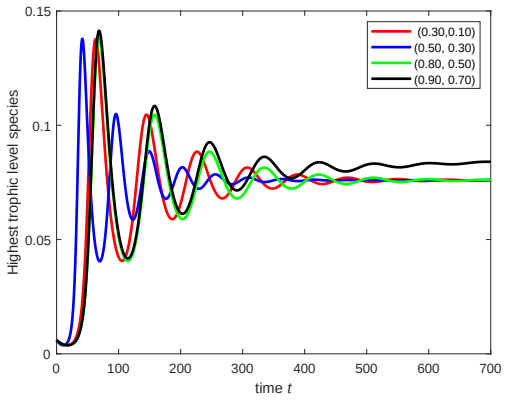

Figure 6. Impact of fractal dimension on the population dynamics of the highest trophic level species in time t.

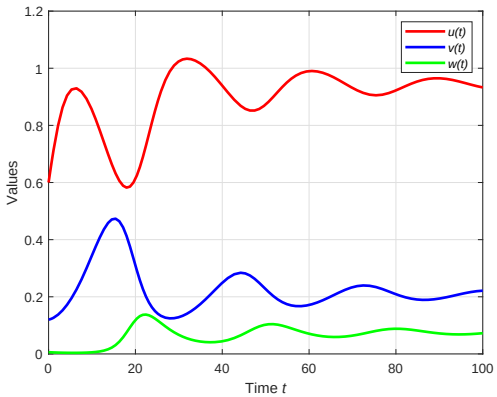

Figure 7. Dynamical behavior of the classical three-species food-chain model.

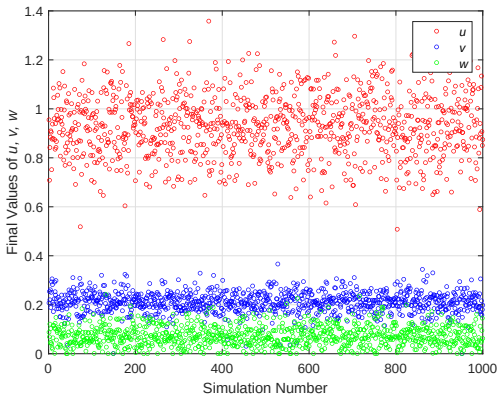

Figure 8. Monte Carlo sensitivity analysis of the lowest, middle, and highest trophic level species.

6. Discussion

In Figures 1–3, we simulate the results for the same fractal dimension but different fractional orders to observe the system's behavior under changes in the fractional order. Similarly, in Figures 4–6, we present simulations for various fractal dimensions and fractional orders to visualize the effect of the fractal dimension. The incorporation of fractional-order derivatives and fractal dimensions exerts a profound influence on the dynamical behavior of the system. Specifically, fractional orders less than unity introduce memory effects that decelerate the evolution of population densities. As the fractional order tends toward unity, the dynamics gradually converge to those governed by classical integer-order differential equations. Concurrently, the inclusion of the fractal dimension serves to modulate the scale and intensity of interspecific interactions, which in turn affects the amplitude and frequency of population oscillations. These parameters provide a versatile framework for adjusting the qualitative behavior of the system.

An extended Adams-Bashforth-Moulton method is adapted to handle the fractal-fractional context. Simulation results confirm that the balance between predation and conversion efficiencies largely determines whether species persist, oscillate, or become extinct. The plot in Figure 8 displays the simulation results of the three-species food chain model, showing the variables u, v, and w over time. Numerical simulations highlight how varying Λ and the fractional order ζ influence convergence rates and oscillatory tendencies. For smaller ζ, slower convergence and longer memory effects are observed, whereas larger ζ produces behaviors closer to classical integer-order systems. In typical scenarios, the prey remains at higher population levels due to its carrying capacity K. The first predator's population fluctuates at intermediate levels, influenced by prey availability and its own mortality rate. The top predator remains at lower levels unless predation rates and conversion efficiencies are fine-tuned to sustain it.

The plot in Figure 8 presents the results of the sensitivity analysis, showing the final values of u, v, and w for each of the 1000 simulations. The x-axis represents the simulation number, while the y-axis represents the final values of the variables. We observe the spread of final values for each variable, where a larger spread indicates higher sensitivity to parameter perturbations. The figure reveals that the final population values of the prey and first predator exhibit greater variability under slight parameter

changes, whereas the top predator shows comparatively lower variability. This suggests that the top predator's survival depends on more stringent conditions, making its population size less sensitive to small parameter fluctuations.

Eigenvalue analysis via the Jacobian matrix shows that the trivial equilibrium is unstable, as the prey's intrinsic growth rate ξ contributes a positive eigenvalue. Biologically, this aligns with the idea that if the prey has a positive growth rate in the absence of predation, its population will not remain at zero. The prey-only equilibrium can be stable if the predators' mortality and predation rates are relatively low or zero, allowing the prey to persist at its carrying capacity. The stability of the prey-first-predator equilibrium depends on thresholds involving predation and mortality rates. If the second predator's impact remains below certain critical values, the system stabilizes at a state where the first predator coexists with the prey while the second predator goes extinct. Full coexistence occurs under a delicate balance of growth, predation, and conversion efficiency parameters for each species. Biologically, this indicates that the top predator can sustain itself if its predation on the middle predator is sufficient but not excessive, preventing the middle predator from going extinct while maintaining viable population levels.

The study employs fixed-point theorems, such as those by Schaefer and Banach, to establish that the model admits a unique solution under suitable conditions on the nonlinear terms and the fractal-fractional derivative parameters. This ensures that the system's dynamics are mathematically consistent, avoiding contradictions or multiple conflicting solutions.

Beyond conventional stability, the study examines Hyers-Ulam (H-U) stability, which ensures that minor deviations in model parameters or initial conditions do not lead to large deviations in solutions. This property is crucial in practical applications where real-world data are subject to measurement errors or small environmental fluctuations.

7. Conclusions

In this study, we develop a tri-trophic food web model that incorporates the carrying capacity of the prey (first species), Holling-type predation of the second species on the first, and subsequent predation of the third species on the second. The novel aspect of this work is the use of the FF-Caputo derivative, which combines the long-memory effect of fractional derivatives with the irregular (fractal) behavior in temporal evolution.

The model has four equilibrium points—trivial equilibrium, prey-only equilibrium, prey-predator equilibrium, and coexistence equilibrium—which we have analyzed graphically. We discuss the stability of these equilibrium points and investigate the existence and uniqueness of the model's solution. Additionally, we derive conditions for its Hyers-Ulam stability in the sense of the FF-Caputo derivative.

Furthermore, we present numerical results and simulations for various fractal and fractional orders. We also simulate the tri-trophic food web model under integer-order conditions, examining the behavior of the variables u, v, and w over time. Lastly, we conduct a sensitivity analysis to evaluate how parameter perturbations affect the final values of the model variables.

This study provides a novel perspective by integrating prudent omnivory and fractal-fractional memory effects into tri-trophic ecological models. The use of the FF-Caputo derivative enhances the model's realism by capturing the non-local memory effect, which is inherent in biological processes

such as delayed response to environmental cues. In practical terms, these insights can support the design of ecosystem management strategies that account for predator selectivity, potentially informing wildlife conservation or sustainable harvesting policies.

Author contributions

Amjad E. Hamza: Writing - review & editing, funding acquisition; Arshad Ali: Writing - original draft; Khaled Aldwoah: Project administration, conceptualization; Hicham Saber: Writing - review & editing; Ria H. Egami: Formal analysis, validation; Amel Towati: Resources, software; Amal F. Alharbi: Validation, visualization. All authors have read and approved the final version of the manuscript for publication.

Use of Generative-AI tools declaration

The authors declare that they have not used Artificial Intelligence (AI) tools in the creation of this article.

Data availability

The paper contains all data that was either created or analyzed throughout the course of this research.

Acknowledgments

The authors extend their appreciation to the Deanship of Scientific Research at Northern Border University, Arar, KSA, for funding this research work through the project number "NBU-FPEJ-2025-2917-02". This study is supported via funding from Prince Sattam bin Abdulaziz University project number (PSAU/2025/R/1446). The authors extend their gratitude to the Islamic University of Madinah.

Conflict of interest

The authors declare that they have no conflicts of interest.

References

1. S. B. Hsu, *A mathematical analysis of competition for a single resource*, Ph.D. Thesis, University of Iowa, 1976.
2. S. B. Hsu, S. Hubbell, P. Waltman, A mathematical theory for single-nutrient competition in continuous cultures of micro-organisms, *SIAM J. Appl. Math.*, **32** (1977), 366–383.
3. P. T. Saunders, M. J. Bazin, On the stability of food chains, *J. Theor. Biol.*, **52** (1975), 121–142. https://doi.org/10.1016/0022-5193(75)90044-2
4. J. A. Yorke, W. N. Anderson, Predator-prey patterns, *Proc. Natl. Acad. Sci. USA*, **70** (1973), 2069–2071. https://doi.org/10.1073/pnas.70.7.2069

5. S. P. Hubbell, Populations and simple food webs as energy filters. II. Two-species systems, *Am. Nat.*, **107** (1973), 122–151.
6. R. M. May, Mass and energy flow in closed ecosystems: A comment, *J. Theor. Biol.*, **39** (1973), 155–163. https://doi.org/10.1016/0022-5193(73)90210-5
7. M. Conrad, Stability of foodwebs and its relation to species diversity, *J. Theor. Biol.*, **34** (1972), 325–335. https://doi.org/10.1016/0022-5193(72)90165-8
8. G. C. Gallopin, Trophic similarity between species in a food web, *Am. Midl. Nat.*, **87** (1972), 336–345. https://doi.org/10.2307/2423566
9. E. H. Kerner, On the Volterra-Lotka principle, *Bull. Math. Biophys.*, **23** (1961), 141–157. https://doi.org/10.1007/BF02477468
10. M. L. Rosenzweig, Exploitation in three trophic levels, *Am. Nat.*, **107** (1973), 275–294. https://doi.org/10.1086/282830
11. D. L. De Angelis, Stability and connectance in food web models, *Ecology*, **56** (1975), 238–243. https://doi.org/10.2307/1935318
12. Y. Ma, R. Yang, Bifurcation analysis in a modified Leslie-Gower with nonlocal competition and Beddington-DeAngelis functional response, *J. Appl. Anal. Comput.*, **15** (2025), 2152–2184. https://doi.org/10.11948/20240415
13. F. Zhu, R. Yang, Bifurcation in a modified Leslie-Gower model with nonlocal competition and fear effect, *Discrete Contin. Dyn. Syst. Ser. B*, **30** (2025), 2865–2893. https://doi.org/10.3934/dcdsb.2024195
14. A. Hastings, T. Powell, Chaos in a three-species food chain, *Ecology*, **72** (1991), 896–903. https://doi.org/10.2307/1940591
15. A. Klebanoff, A. Hastings, Chaos in three species food chains, *J. Math. Biol.*, **32** (1994), 427–451. https://doi.org/10.1007/BF00160167
16. A. Rescigno, K. G. Jones, The struggle for life: III. A predator-prey chain, *Bull. Math. Biophys.*, **34** (1972), 521–532. https://doi.org/10.1007/BF02476712
17. A. R. Hausrath, Stability properties of a class of differential equations modeling predator-prey relationships, *Math. Biosci.*, **26** (1975), 267–281. https://doi.org/10.1016/0025-5564(75)90016-4
18. V. Seralan, R. Vadivel, N. Gunasekaran, T. Radwan, Dynamics of fractional-order three-species food chain model with vigilance effect, *Fractal Fract.*, **9** (2025), 45. https://doi.org/10.3390/fractalfract9010045
19. S. Pal, P. K. Tiwari, A. K. Misra, H. Wang, Fear effect in a three-species food chain model with generalist predator, *Math. Biosci. Eng.*, **21** (2024), 1–33. https://doi.org/10.3934/mbe.2024001
20. T. K. Kar, Stability analysis of a prey-predator model incorporating a prey refuge, *Commun. Nonlinear Sci. Numer. Simul.*, **10** (2005), 681–691. https://doi.org/10.1016/j.cnsns.2003.08.006
21. S. Pal, A. Gupta, A. K. Misra, B. Dubey, Chaotic dynamics of a stage-structured prey-predator system with hunting cooperation and fear in presence of two discrete delays, *J. Biol. Syst.*, **31** (2023), 611–642. https://doi.org/10.1142/S0218339023500213

22. Sajan, K. K. Choudhary, B. Dubey, A non-autonomous approach to study the impact of environmental toxins on nutrient-plankton system, *Appl. Math. Comput.*, **458** (2023), 128236. https://doi.org/10.1016/j.amc.2023.128236

23. A. Gupta, B. Dubey, Role reversal in a stage-structured prey-predator model with fear, delay, and carry-over effects, *Chaos*, **33** (2023), 093114. https://doi.org/10.1063/5.0160222

24. H. I. Freedman, P. Waltman, Mathematical analysis of some three-species food-chain models, *Math. Biosci.*, **33** (1977), 257–276. https://doi.org/10.1016/0025-5564(77)90142-0

25. A. Gupta, S. Sajan, B. Dubey, Chaos in a seasonal food-chain model with migration and variable carrying capacity, *Nonlinear Dyn.*, **112** (2024), 13641–13665. https://doi.org/10.1007/s11071-024-09718-1

26. A. Atangana, Fractal-fractional differentiation and integration: Connecting fractal calculus and fractional calculus to predict complex system, *Chaos Solitons Fract.*, **102** (2017), 396–406. https://doi.org/10.1016/j.chaos.2017.04.027

27. K. Shah, T. Abdeljawad, Study of radioactive decay process of uranium atoms via fractals-fractional analysis, *S. Afr. J. Chem. Eng.*, **48** (2024), 63–70. https://doi.org/10.1016/j.sajce.2024.01.003

28. A. Shah, H. Khan, M. De la Sen, J. Alzabut, S. Etemad, C. T. Deressa, et al., On non-symmetric fractal-fractional modeling for ice smoking: Mathematical analysis of solutions, *Symmetry*, **15** (2022), 87. https://doi.org/10.3390/sym15010087

29. M. Riaz, F. A. Alqarni, K. Aldwoah, F. M. O. Birkea, M. Hleili, Analyzing a dynamical system with harmonic mean incidence rate using Volterra-Lyapunov matrices and fractal-fractional operators, *Fractal Fract.*, **8** (2024), 321. https://doi.org/10.3390/fractalfract8060321

30. M. Arfan, H. Alrabaiah, M. U. Rahman, Y. L. Sun, A. S. Hashim, B. A. Pansera, et al., Investigation of fractal-fractional order model of COVID-19 in Pakistan under Atangana-Baleanu Caputo (ABC) derivative, *Results Phys.*, **24** (2021), 104046. https://doi.org/10.1016/j.rinp.2021.104046

31. S. Djilali, C. Cattani, L. N. Guin, Delayed predator-prey model with prey social behavior, *Eur. Phys. J. Plus*, **136** (2021), 940. https://doi.org/10.1140/epjp/s13360-021-01940-9

32. S. Khajanchi, Dynamic behavior of a Beddington-DeAngelis type stage structured predator-prey model, *Appl. Math. Comput.*, **244** (2014), 344–360. https://doi.org/10.1016/j.amc.2014.06.109

33. P. Panday, N. Pal, S. Samanta, P. Tryjanowski, J. Chattopadhyay, Dynamics of a stage-structured predator-prey model: Cost and benefit of fear-induced group defense, *J. Theor. Biol.*, **528** (2021), 110846. https://doi.org/10.1016/j.jtbi.2021.110846

34. R. Kaushik, S. Banerjee, Predator-prey system: Prey's counter-attack on juvenile predators shows opposite side of the same ecological coin, *Appl. Math. Comput.*, **388** (2021), 125530. https://doi.org/10.1016/j.amc.2020.125530

35. K. Latrach, M. A. Taoudi, A. Zeghal, Some fixed point theorems of the Schauder and the Krasnosel'skii type and application to nonlinear transport equations, *J. Differ. Equ.*, **221** (2006), 256–271. https://doi.org/10.1016/j.jde.2005.04.010

36. B. Ahmad, S. K. Ntouyas, A. Alsaedi, New existence results for nonlinear fractional differential equations with three-point integral boundary conditions, *Adv. Differ. Equ.*, **2011** (2011), 107384. https://doi.org/10.1155/2011/107384

37. B. C. Dhage, S. B. Dhage, K. Buvaneswari, Existence of mild solutions of nonlinear boundary value problems of coupled hybrid fractional integro-differential equations, *J. Fract. Calc. Appl.*, **10** (2019), 191–206.

38. A. Devi, A. Kumar, Hyers-Ulam stability and existence of solution for hybrid fractional differential equation with p-Laplacian operator, *Chaos Solitons Fract.*, **156** (2022), 111859.

39. H. Vu, J. M. Rassias, N. V. Hoa, Hyers-Ulam stability for boundary value problem of fractional differential equations with ψ-Caputo fractional derivative, *Math. Methods Appl. Sci.*, **46** (2023), 438–460. https://doi.org/10.1002/mma.8520

40. M. S. Algolam, O. Osman, A. Ali, A. Mustafa, K. Aldwoah, A. Alsulami, Fixed point and stability analysis of a tripled system of nonlinear fractional differential equations with n-nonlinear terms, *Fractal Fract.*, **8** (2024), 697. https://doi.org/10.3390/fractalfract8120697

41. M. A. Khan, A. Atangana, *Numerical methods for fractal-fractional differential equations and engineering simulations and modeling*, CRC Press, 2023. https://doi.org/10.1201/9781003359258